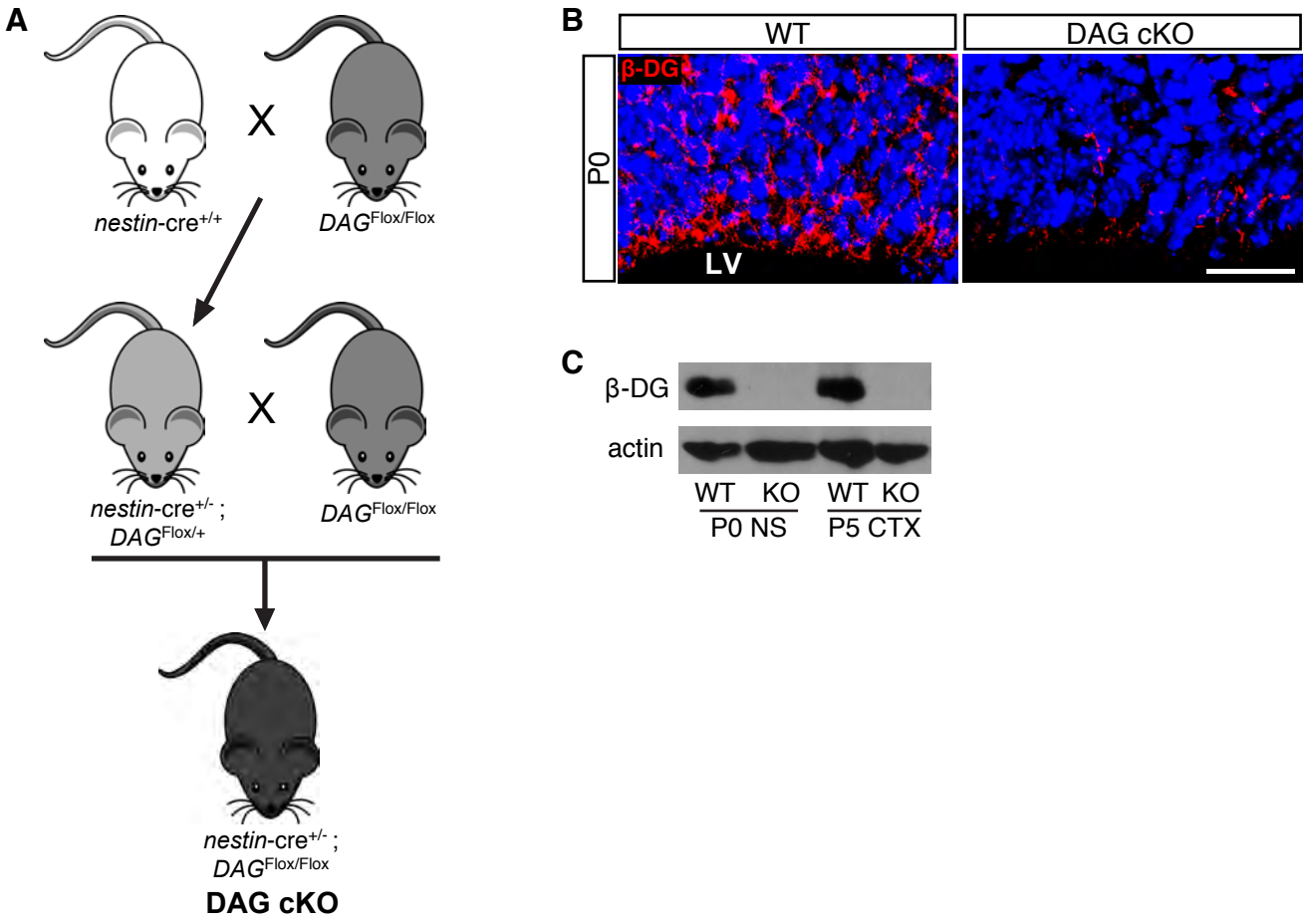

Figure S1. McClenahan et al.

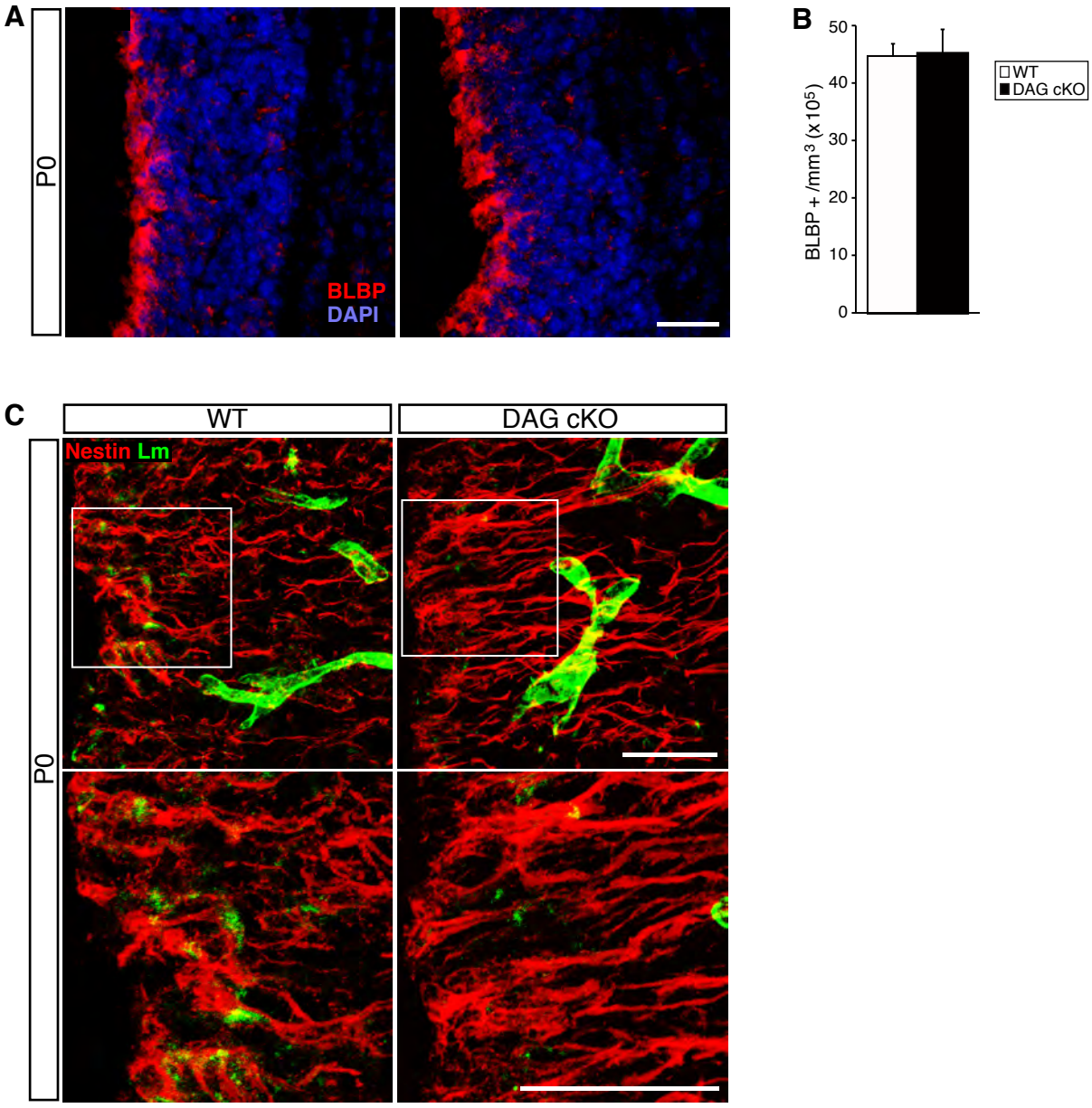

Figure S2. McClenahan et al.

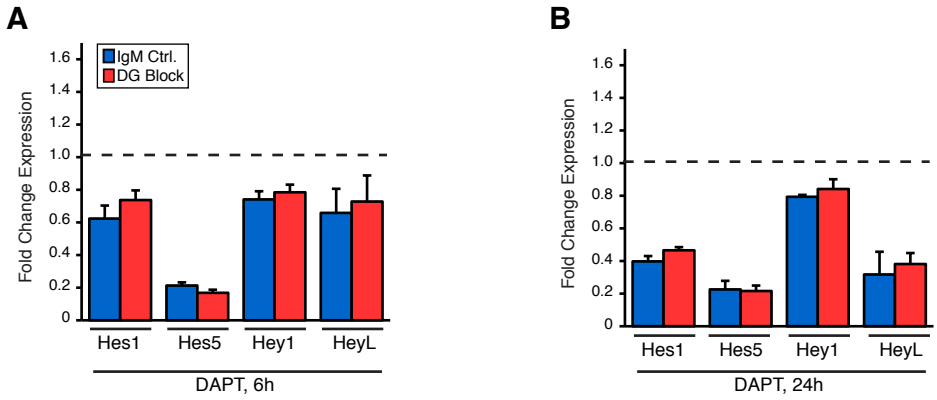

Figure S3. McClenahan et al.

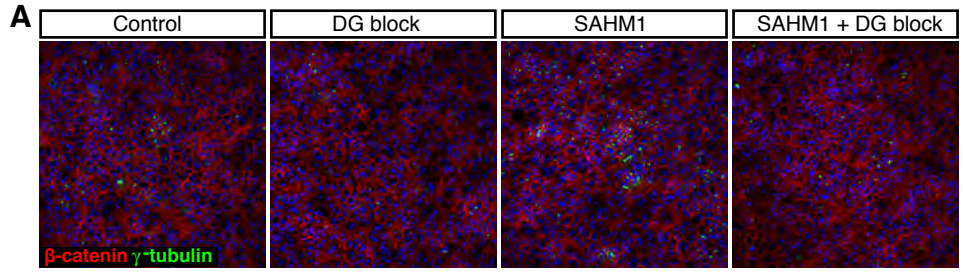

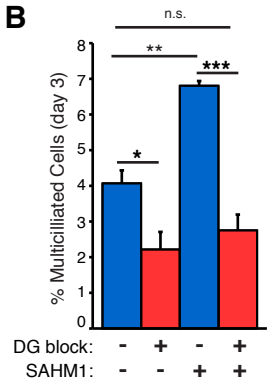

Figure S4. McClenahan et al.

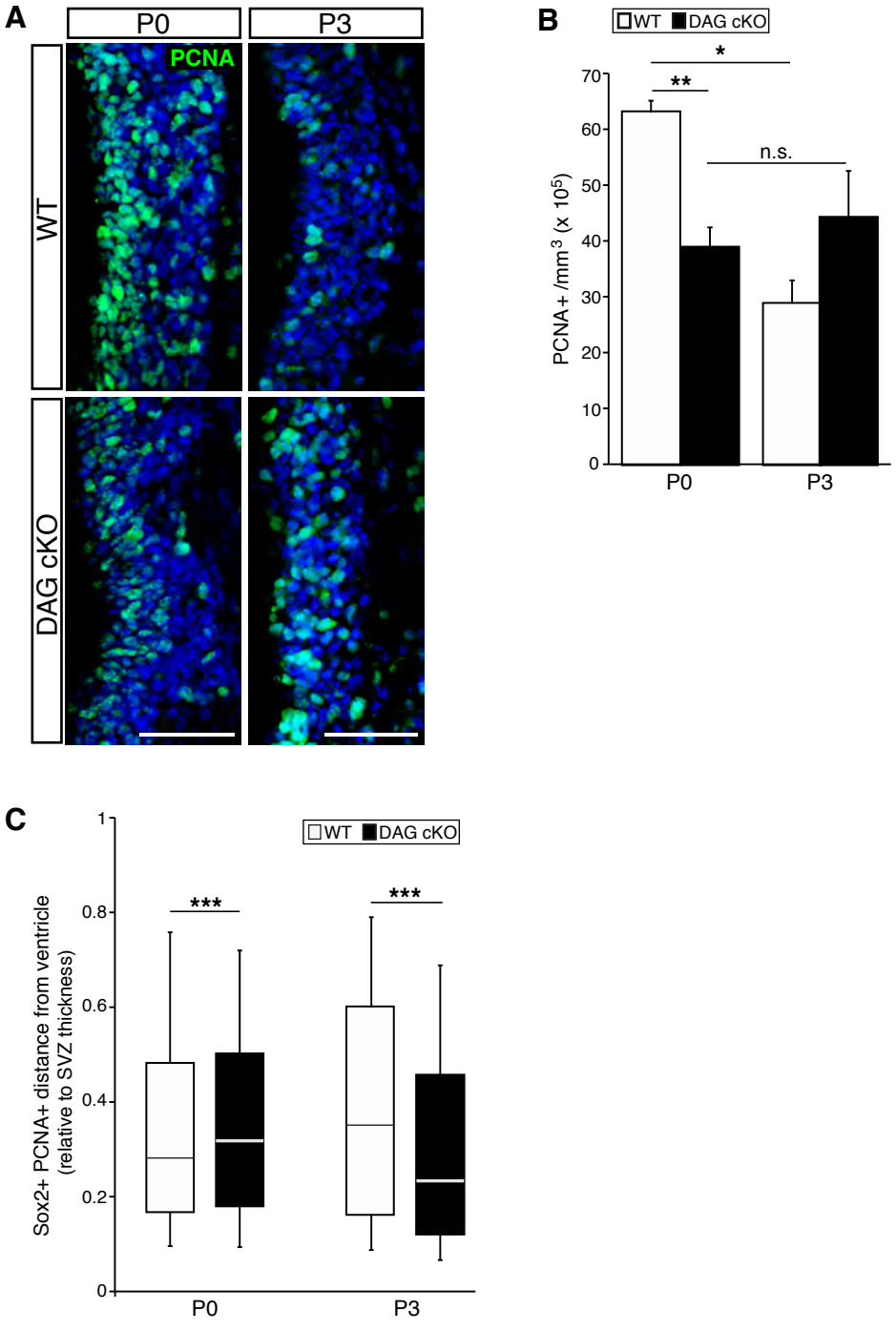

Figure S5. McClenahan et al.

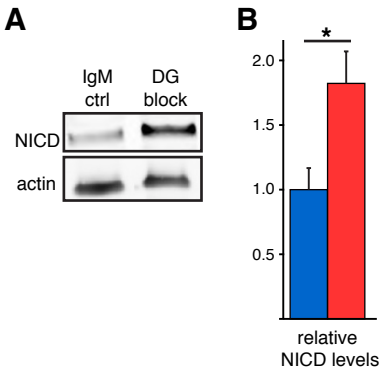

Figure S6. McClenahan et al.

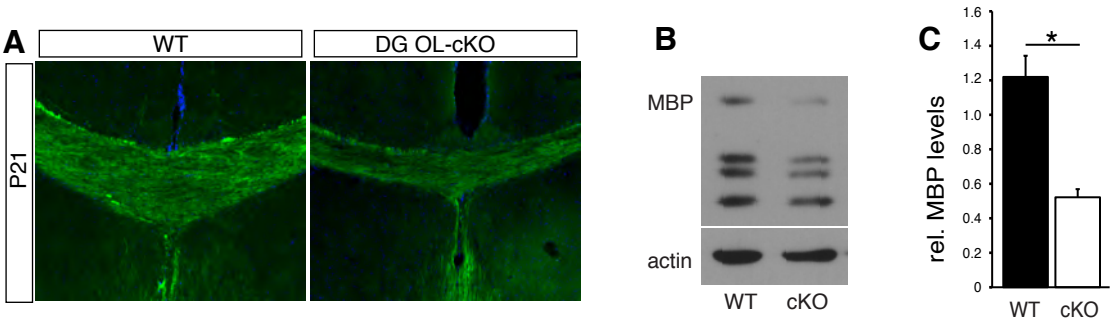

Figure S7. McClenahan et al.

Supplemental Figure Legends

Figure S1. Confirmation of dystroglycan loss in conditional knockout mouse model (related to Figure 2). Generation of *Nestin*-cre^{+}; *DAG*$^{Flox/Flox}$ (DAG cKO) mice. (A) Schematic of breeding scheme used obtain *Nestin*-cre^{+};*DAG*$^{Flox/Flox}$ (DAG cKO) mice. (B) IHC against β-dystroglycan in coronal sections taken from P0 WT and DAG cKO mice. Scale bar: 25 μm. (C) Western blotting against β-dystroglycan on lysates taken from i) second passage neurospheres isolated from P0 WT and DAG cKO mice and ii) cortices from P5 WT and DAG cKO mice.

Figure S2. Perinatal radial glia in DAG cKO mice (related to Figure 3). (A) IHC to detect BLBP in coronal sections from P0 WT and DAG cKO mice. Perinatal WT and DAG cKO mice had similar BLBP+ radial glial cell densities. (B) Quantification of BLBP+ cell density at P0 in WT and DAG cKO mice. (C) IHC to detect nestin and laminin (Lm) in coronal sections from P0 WT and DAG cKO mice. In WT mice, the apical processes of nestin+ radial glia make contact with laminin puncta at the ventricular surface. In DAG cKO mice there were fewer laminin-positive puncta and radial glial association with the remaining puncta was reduced. The association of radial glial basal processes with SVZ blood vessels did not appear to be altered in DAG cKO mice. Error bars, SEM; n=3. Scale bars: 25 μm.

Figure S3. DAPT blocks canonical Notch signaling in the presence or absence of dystroglycan-blocking antibodies (related to Figure 4). (A) Fold change in mRNA levels of *Hes1*, *Hes5*, *Hey1*, and *HeyL* in confluent SVZ ependymal cultures at 6 post-switch to maturation medium, in the presence or absence of the γ-secretase inhibitor, DAPT, or dystroglycan (DG)-blocking antibodies. (B) Experiment as in (A) but mRNA was analyzed at 24 hours post-treatment (error bars, SEM; n=6).

Figure S4. SAHM1 peptide influence on ependymal cell cultures (related to Figure 4). (A) IHC to detect β-catenin and γ-tubulin in SVZ ependymal cell cultures at day 3 in maturation medium. While in maturation medium, cultures were treated with the Notch inhibitor SAHM1, dystroglycan-blocking antibodies (DG block), or a combination thereof.

(B) The percentage of cells reaching a multiciliated phenotype by day 3 differentiation. SAHM1 treatment increased the percentage of SVZ cells acquiring a multiciliated phenotype, and DG-blocking antibody decreased the percentage of SVZ cells acquiring a multiciliated phenotype. However, cells with a combination of both SAHM1 and DG block were not significantly (n.s.) different compared to control cells (*p<0.05, **p<0.01, ***P<0.001, Student's t-test; error bars, SEM; n=4).

Figure S5. Neural stem and progenitor cell proliferation is dysregulated in the DAG cKO SVZ (related to Figure 5). (A) IHC to detect PCNA in coronal sections from P0 and P3 WT and DAG cKO mice. (B) Quantification of PCNA+ cell density in the SVZ of WT and DAG cKO mice at P0 and P3 (*p < 0.05, **p < 0.01, Student's t-test; error bars, SEM; n=3). While proliferation in WT mice is high at P0 and decreases sharply by P3, proliferation in the DAG cKO SVZ is greatly reduced at P0 and does not change significantly from P0 to P3. (C) Quantification of sox2+ PCNA+ nuclear distance from the lateral ventricle, relative to total SVZ thickness, in P0 WT and DAG cKO mice (***p < 0.001, Wilcoxon rank sum test; error bars, 1.5 IQR; n=3).

Figure S6. NICD levels are elevated in SVZ cultures treated with dystroglycan-blocking antibodies (related to Figure 5). (A) NICD western blots of protein lysates obtained from neonatal SVZ ependymal cultures after 3 days in medium to promote ependymal cell differentiation. (B) Cultures with dystroglycan (DG)-blocking antibodies had increased levels of NICD protein relative to actin, compared to cultures treated with control antibodies (*p<0.05, Student's t-test; error bars, SEM; n=9).

Figure S7. Myelin basic protein levels are increased in the DAG OL-cKO corpus callosum (related to Figure 6). (A) IHC to detect myelin basic protein (MBP) in the corpus callosum in coronal sections from P21 WT and DAG OL-cKO mice. MBP immunoreactivity is decreased in DAG OL-cKO mice. Scale bars: 100 μm. (B) Western blot analyses of MBP protein levels in cortical lysates from WT and DAG OL-cKO mice at P21. (C) Quantification of relative MBP protein levels in cortical lysates from WT and DAG OL-cKO mice at P21 (*p<0.05; Student's t-test; error bars, SEM; n=4).

Supplemental Experimental Procedures

Primary Antibodies

Rabbit anti- γ-tubulin (Sigma-Aldrich T5192, 1:500), mouse anti-β-catenin (BD Transduction 610153, 1:500), mouse IgM anti-α-Dystroglycan, clone IIH6C4 (Upstate Cell Signaling 05-593, 1:50- 1:100), mouse anti-PCNA (Cell Signaling Technology, 1:200), rabbit anti-Sox2 (Millipore AB5603, 1:100), chicken anti-Nestin (Aves Labs NES, 1:500), mouse anti-Nestin (Developmental Studies Hybridoma Bank Rat-401, 1:5), rat anti-MBP (Serotec MCA409S, 1:100), mouse anti-CNPase (Sigma C5922, 1:100), rabbit anti-NG2 (Chemicon International AB5320, 1:200), mouse anti-APC (CC-1) (Calbiochem OP80, 1:100), rabbit anti-GFAP (DakoCytomation Z0334, 1:500), rat anti-PDGFRα (CD140a) (BD Pharmingen 558774, 1:100), rabbit anti-PDGFRα (Santa Cruz SC-338, 1:150), rabbit anti-Laminin (Sigma L9393, 1:100), chicken anti-GFP(Aves GFP, 1:500), rat anti-CD24 (BD Biosciences 557436, 1:100-1:200), rabbit anti-notch ICD for IHC (Abcam), mouse anti-notch ICD for western (Developmental Studies Hybridoma Bank).

Primers

Myb: 5'-AGCAGGCATTACCAACACAGA-3' and 5'-CTGCTGAGATCACACCACGA-3'; *FoxJ1*: 5'-CTTCCGCCATGCAGACCCCA-3' and 5'-CGGGCAAAGGCAGGGTGGAT-3'; *Notch1*: 5'-AGTGCAACCCCCTGTATGAC-3' and 5'-TCTAGGCCATCCCACTCACA-3'; *Numb*: 5'-GGCTTCTTTGGAAAAACGGGA-3' and 5'-CTCAGTCTTTCCCCCGTGTC3'; *MCIDAS*: 5'GGCCTCAGTGCTGGATAAGC-3' and 5'-TAGGGTCACGATTGTGCAGG-3'; *Jagged1*: 5'- ATA CAC GTG GCC ATC TCT GC-3' and 5'-CCG CTT CCT TAC ACA CCA GT-3'; *Jagged2*: 5'- TGC CTC TAA CCC ATG TGC AG – 3' and 5'- TCA CAC TCA TTG GCG TCC AG-3'; *Dll1*: 5'- ACC AAG TGC CAG TCA CAG AG-3' and 5'- TCC ATC TTA CAC CTC AGT CGC – 3'; *Dll3*: 5' - GGG CAG CTG TAG TGA AAC CT-3' and 5'-CTT CAC CGC CAA CAC ACA AG-3'; *Dll4*: 5' - GTG GCA GCT GTA AGG ACC A – 3' and 5'- CGC GCA GGT CAA GGT ACT AT-3'; *Olig2*: 5' - TTA CAG ACC GAG CCA ACA CC – 3' and 5'- TCA ACC TTC CGA ATG TGA ATT AGA -3'; *Mash1*: 5' - GAA TGG ACT TTG GAA GCA GGA TG-3' and 5'- CAT TTG ACG TCG TTG GCG AG- 3';

Sox9: 5’ - CAC AAG AAA GAC CAC CCC GA – 3’ and 5’- GGA CCC TGA GAT TGC CCA GA-3’; *Hes5*: 5’ - CAA GGA GAA AAA CCG ACT GCG – 3’ and 5’ - GCG AAG GCT TTG CTG TGT TT – 3’; *HeyL*: 5’ - GAA GAA GCG CAG AGG GAT CA – 3’ and 5’ - AGG CAT TCC CGA AAC CCA AT – 3’; 5’-*Hes1*: CTACCCCAGCCAGTGTCAAC-3’ and 5’-ATGCCGGGAGCTATCTTTCT-3’; *Hey1*: 5’- TACCCAGTGCCTTTGAGAAG-3’ and 5’-AACCCCAAACTCCGATAGTC-3’